

# **Forecast experiments with the ALADIN 3D-FGAT analysis system**

Sándor Kertész

Hungarian Meteorological Service

## 1. Introduction

The FGAT (First Guess at Appropriate Time) technique was first implemented in the ECMWF optimal interpolation analysis system (ECMWF, 1992). Its extension to variational data assimilation, the so-called 3D-FGAT system, is regarded as an intermediate step between 3D-VAR and 4D-VAR. In contrast to 3D-VAR, which cannot handle temporal information and is restricted to the analysis time, 3D-FGAT is even able to take into account the temporal distribution of the observations (though only in a limited way). The 3D-FGAT scheme was operationally used at different forecast centres (e.g. at the ECMWF) and it is still an operational option for HIRLAM (Huang *et al.*, 2002). The work with the ALADIN 3D-FGAT system started only a couple of years ago (Soci, 2004) and up to now only a few experiments have been carried out (Dziedzic, 2005, Vasiliu, 2006).

In this paper the recent research studies devoted to the ALADIN 3D-FGAT system at the Hungarian Meteorological Service (HMS) are presented. These studies focused on three main topics. At first, the choice of the temporal position of the 3D-FGAT analysis increment was investigated. It was followed by a comparison of the 3D-VAR and 3D-FGAT systems. Finally the possible usage of all the available SYNOP reports in the observation window was tested.

## 2. Theoretical background

The 3D-FGAT system can be best described as a simplification of 4D-VAR. In 4D-VAR the analysis is performed for a time interval (observation window) and the result is the trajectory that lies closest to both the  $\mathbf{x}_b$  background state (specified at the beginning of the observation window) and the  $\mathbf{y}$  observations. In practice the observation window is divided into  $n$  time-slots and all the observations within a given time-slot are supposed to be valid at the middle of the time-slot. In the incremental formalism of 4D-VAR the analysis is yielded by the minimization of a  $J$  cost function with respect to the  $\delta \mathbf{x} = \mathbf{x} - \mathbf{x}_b$  analysis increment. The cost function takes the following form:

$$J(\delta \mathbf{x}) = \delta \mathbf{x}^T \mathbf{B}^{-1} \delta \mathbf{x} + \sum_{i=1}^n (\mathbf{d}_i - \mathbf{H} \delta \mathbf{x}_i)^T \mathbf{R}^{-1} (\mathbf{d}_i - \mathbf{H} \delta \mathbf{x}_i)$$

where

- $\mathbf{B}$  is the background error covariance matrix,
- $\mathbf{R}$  is the observation error covariance matrix,
- $\mathbf{H}$  is the tangent linear operator of the  $H$  observation operator,
- $M_i(\mathbf{x}_b)$  is the background trajectory computed by the  $M$  forecast model,
- $\mathbf{d}_i = \mathbf{y}_i - H(M_i(\mathbf{x}_b))$  is the innovation vector that gives the departure between the observations and the background trajectory,
- $\delta \mathbf{x}_i = \mathbf{M}_i \delta \mathbf{x}$  is the increment propagated forward in time with the  $\mathbf{M}$  tangent linear operator of the forecast model. Both  $H$  and  $M$  are linearised along the background trajectory.

This minimization problem is solved by an iterative process that in each step requires the evaluation of the  $J$  cost function and its  $\nabla J$  gradient. Throughout the iterations the  $\mathbf{d}$  innovation vector is constant (it has to be computed only once) but in each iteration step the integration of the  $\mathbf{M}$  tangent linear model and its  $\mathbf{M}^T$  adjoint is required making 4D-VAR computationally expensive.

The computational costs and the scientific complexity of the problem can be greatly reduced by using the 3D-FGAT algorithm that we get from 4D-VAR by setting the tangent linear model operator and its adjoint to the identity  $\mathbf{M} = \mathbf{M}^T = \mathbf{I}$ . This means that  $\delta \mathbf{x}_i = \delta \mathbf{x}$  so in 3D-FGAT the following cost function has to be minimized:

$$J(\delta \mathbf{x}) = \delta \mathbf{x}^T \mathbf{B}^{-1} \delta \mathbf{x} + \sum_{i=1}^n (\mathbf{d}_i - \mathbf{H} \delta \mathbf{x})^T \mathbf{R}^{-1} (\mathbf{d}_i - \mathbf{H} \delta \mathbf{x})$$

It can be seen that in 3D-FGAT we still have the background trajectory and the innovation vector is computed correctly (the name FGAT comes from this fact) but the temporal information in the increment is completely lost. As a consequence the incremental 3D-FGAT analysis is ambiguous since the resulting analysis increment is not fixed in time and theoretically it can be added at any time position to the background trajectory.

Further simplification of the minimization problem, by removing all the temporal information from the system, results in the 3D-VAR algorithm with the following cost function:

$$J(\delta \mathbf{x}) = \delta \mathbf{x}^T \mathbf{B}^{-1} \delta \mathbf{x} + (\mathbf{d} - \mathbf{H} \delta \mathbf{x})^T \mathbf{R}^{-1} (\mathbf{d} - \mathbf{H} \delta \mathbf{x})$$

In 3D-VAR everything refers to the analysis time that is usually the middle of the observation window. All the observations in the observation window are supposed to be valid at this time and there is no background trajectory, instead the background is also specified at the middle of the observation window.

### 3. Theoretical aspects of observation handling in 3D-FGAT

The 3D-FGAT system is thought to be more advanced than 3D-VAR due to its more precise observation handling. However, this takes effect only if there are observations at different times than the analysis time, otherwise the two systems give identical results. Concerning the temporal-spatial distribution of these observations two major cases can be distinguished:

1. The observing platform is moving. There can be cases when there is only one observation for a given location in the observation window. An example for it is a sensor on a quasi-polar satellite. With other moving platforms it can happen that in the vicinity of certain locations there are a plenty of observations at different times. This is the case of the aircraft-based observations (AIREP reports).
2. The observation platform is fixed and there are more measurements within the observation window like for the land SYNOP observations. In this case there can be more observations at exactly the same location but with different observation times.

The theoretical investigation of these cases is quite easy if there is only one observation location for the whole analysis. Let us suppose at first that we have only one  $y$  observation for a model variable and it is located at a given model grid point. With these assumptions the observation operator directly assigns some  $k$ -th element of the model space to the observation, so the innovation can be written as  $d = y - (\mathbf{x}_b)_k$  and the resulting 3D-FGAT analysis increment takes the following form:

$$(\delta \mathbf{x})_k = \frac{\sigma_{bk}^2}{\sigma_o^2 + \sigma_{bk}^2} d$$

where

- $\sigma_{bk}$  is the background error variance for point  $k$  in the model space,
- $\sigma_o$  is the observation error for the given observation.

Obviously, the 3D-VAR analysis would yield the same increment but with a less accurately computed  $d$  innovation if the observation is far from the analysis time. This may indicate the clear

advantage of 3D-FGAT over 3D-VAR for example for a sensor of a polar satellite (as it was described above).

Let us suppose now that we have one observation with the conditions mentioned above in each of the  $n$  timeslots. Then the  $k$ -th element of the 3D-FGAT analysis increment can be written as:

$$(\delta \mathbf{x})_k = \frac{\sigma_{bk}^2}{\frac{\sigma_o^2}{n} + \sigma_{bk}^2} \frac{1}{n} \sum_{i=1}^n d_i$$

If these observations would be assimilated with 3D-VAR then the increment would have the same form again (supposing that  $\mathbf{R}$  is diagonal) but it would be based on completely wrong  $d_i$  innovation values. This formula means that the increment is yielded as if the average background departure were taken into account with a decreased observation error. As we mentioned this can be the case of the land SYNOP reports and also to a certain extent of the AIREP reports. Concerning these observation types it is not clear from the formulae presented above which solution produces better result in 3D-FGAT: using only one observation at (or around) a certain location at the analysis time or using a kind of averaging by taking more observations at different times.

#### 4. Implementation of 3D-FGAT in ALADIN

The implementation of the incremental 3D-FGAT system in ALADIN/ARPEGE/IFS follows the scheme described in Chapter 2, i.e. 3D-FGAT is equivalent with an outer loop of 4D-VAR where the tangent linear model and its adjoint is set to the identity operator. From the practical point of view an ALADIN 3D-FGAT run is rather similar to a 3D-VAR one. Both systems require the same steps such as observation pre-processing, observation screening (configuration 002) and minimization (configuration 131), but there are some relevant differences:

- In the observation pre-processing the main difference is that in 3D-FGAT the observation window is divided into time-slots. Time-slots must be defined during the observation pre-processing and an ODB (Observational DataBase) with timeslots has to be created.
- The screening in 3D-FGAT works with the background trajectory and the innovation vectors (i.e. background departures) are computed using the appropriate observation times. So the quality control using these departures is more accurate than in 3D-VAR. The background trajectory is computed by the screening itself. This model integration is started from the  $\mathbf{x}_b$  background state. This means that the background state is always specified at the beginning of the observation window in contrast to 3D-VAR where it is valid at the middle of the window. Practically 3D-FGAT runs the same screening as 4D-VAR.
- The minimization in 3D-FGAT also performs one model integration and computes the background trajectory again. In the end of the minimization the resulting analysis increment is added to the background trajectory at the beginning of the observation window, this is the hard-coded setting.

Concerning the computational costs a 3D-FGAT run requires an extra CPU time only for the computation of the background trajectory. The minimization itself in 3D-FGAT is only a slightly slower than in 3D-VAR.

#### 5. Description of the experiments

The experiments were carried out for the period of 4-21 May, 2005 with the ALADIN CY28T3 model version using a 12 km horizontal resolution with 37 vertical levels (up to 5 hPa).

The integration domain is shown on Figure 1. In each experiment a 6 hour assimilation cycle with a  $\pm 3$  hour observation window was used and two 48 hour model integrations were performed at 00 and 12 UTC. The first 4 days of the investigated period was regarded as a warm-up time and forecasts were run only for the remaining two weeks of the period (8-21 May). The same B-matrix (standard NMC) and statistics (e.g. bias correction coefficients) were used both in 3D-VAR and 3D-FGAT. Instead of having a surface analysis the surface fields from the ARPEGE analyses (or forecasts) were copied into the ALADIN background. In the 3D-FGAT experiments the 6 hour observation window was divided into 7 one hour time-slots starting at -3:30 h and ending at +3:30 h relating to the middle of the window.

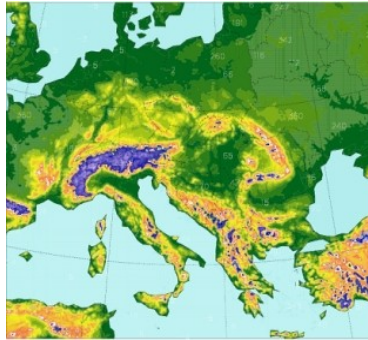


Figure 1: The integration domain and orography of the ALADIN model

In the experiments all observation types available at HMS were used: land SYNOP, AIREP, AMV winds (from MSG), TEMP, Wind profiler observations and NOAA AMSU-A and AMSU-B sensors. The characteristics of the reference set of observations are shown in Table 1. Beside these observations additional parameters and observation times were used in some of the experiments.

<i>Observations</i>	<i>Parameters</i>	<i>Temporal usage</i>
SYNOP (land)	Z	one report per station (closest to the analysis time)
AIREP	U, V, T (thinning: 25 km)	all the reports in the observation window
AMV	U, V (thinning: 25 km)	observations 15 minutes before the analysis time
TEMP	T, U, V, Q, Z	one report per station (closest to the analysis time)
Wind profiler	U, V	one report per station (closest to the analysis time)
AMSU A,B	T <sub>b</sub> (thinning: 80 km)	all the reports in the observation window

Table 1: The reference set of observations used in the experiments

## 6. The timing of the analysis increment in 3D-FGAT

In the first set of experiments the timing of the analysis increment was investigated. As we described above, the ALADIN model adds the increment to the background trajectory at the beginning of the observation window. It means that with a 6 hour analysis scheme 3D-FGAT analyses are available at 03, 09, 15 and 21 UTC and in order to have a 48 hour forecast from e.g. 00 UTC we have to run a 54 hour forecast from 21 UTC. This scheme (illustrated on Figure 2a) was tested and proved to be insufficient comparing to 3D-VAR (Vasiliiu, 2006). One of the reason of this feature could be the extra 3 hours of integration that can spoil the information in the analysis. Another idea was that TEMP observations, which have huge impact on analysis quality, are located at the middle of the observation window but with this scheme their effect is taken into account 3 hours before. Therefore it was thought that the increment should be added to the background

trajectory at the middle of the assimilation window. This modified cycling scheme (that was implemented by adding the increment to the trajectory by an external program) can be seen on Figure 2b.

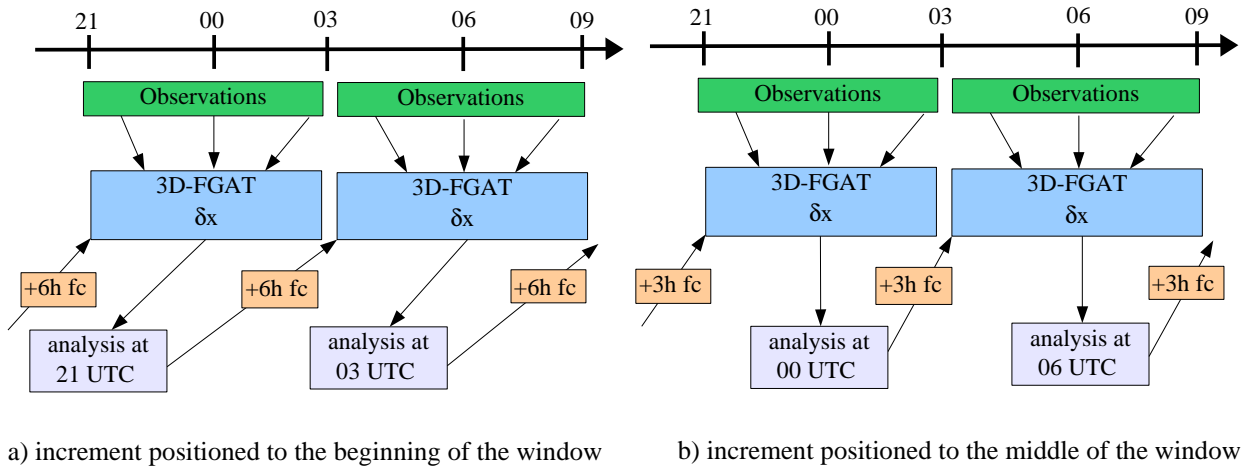


Figure 2: The two cycling schemes of 3D-FGAT that were tested: using the default increment position at the beginning of the observation window (Figure a, on the left), and adding the increment to the background trajectory at the middle of the observation window (Figure b, on the right).

In order to test these schemes two 3D-FGAT experiments were performed using the reference set of observations (see Table 1). The comparison of the forecasts clearly showed that the increment should be added to the background trajectory at the middle of the observation window: in this case the verification scores are significantly better for both the surface and upper air parameters (Figure 3). Thus, all the 3D-FGAT experiments presented in the rest of this report were performed using this scheme.

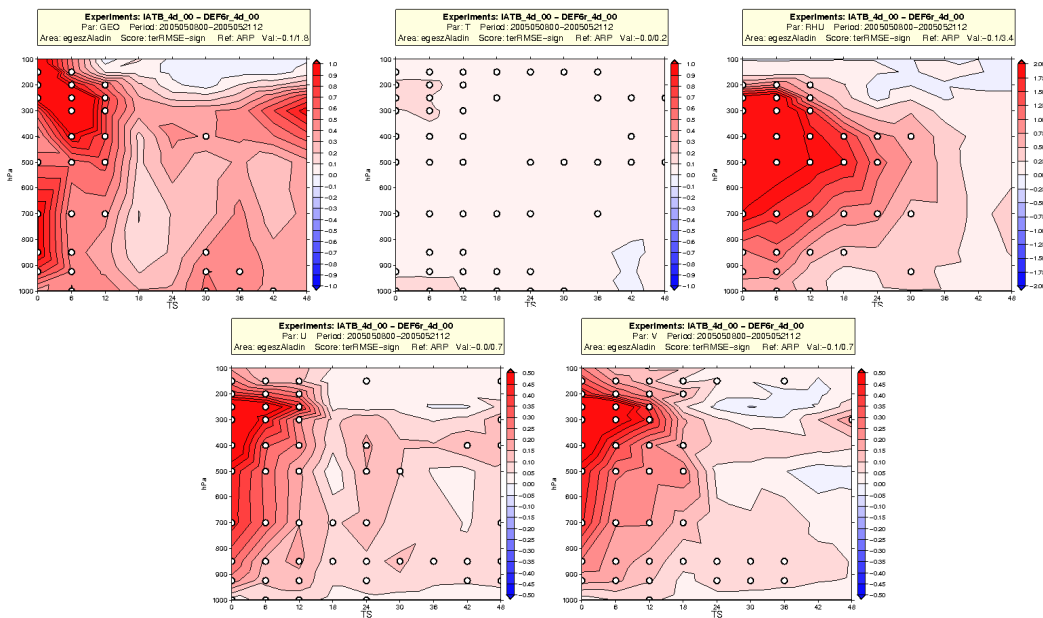


Figure 3.: Difference of RMSE scores of the 00 UTC forecasts based on the original (increment at the beginning of the window) and the modified (increment in the middle of the window) 3D-FGAT cycling schemes. Red shades indicate that the new scheme is better, while blue shades indicate the opposite. White circles show that the difference is significant on a 90% confidence level. The verification was performed against ARPEGE analyses. The figure order is the following (from left to right): Z, T, RHU, U and V.

## 7. Comparing 3D-FGAT with 3D-VAR

For the sake of the correct comparison of 3D-FGAT with 3D-VAR the 6 hour analysis cycling in 3D-VAR started (at 00 UTC, 4 May) from the 3 hour forecast made by the 3D-FGAT screening. So for the first analysis the background state of 3D-VAR and the middle point of the background trajectory of 3D-FGAT (where the increment is positioned to) were the same. These experiments consisted of two parts: at first the reference set of observations were used, then the usage of a shorter ( $\pm 1$  hour) observation window for AIREP both in 3D-VAR and 3D-FGAT was investigated.

### 7.1 Reference experiments

In these experiments the reference set of observations (see Table 1) was used with a 6h observation window. It means that with the exception of AIREP reports and satellite radiances all the observations were available at the analysis time. As a consequence, the difference between 3D-VAR and 3D-FGAT must be the result of the different handling of these two observation types.

#### 7.1.1 Comparison of observation handling

The comparison of the observation handling was carried out by the investigation of the background departures. The analysis departures could have been also investigated, however due to the timing problems with the 3D-FGAT analysis increment this comparison was rather ignored. The screening quality control (observations finally get active or rejected status) was also studied because some of the screening tests are based on the background departures. Therefore it was expected that for observations far from the analysis time 3D-FGAT (due to its more precise background departure computation) would reject less observations than 3D-VAR. The results are presented in Table 2.

		<i>Total</i>	<i>Rejected</i>		<i>Obs-Guess Mean</i>		<i>Obs-Guess STD</i>	
			<i>3D-VAR</i>	<i>3D-FGAT*</i>	<i>3D-VAR</i>	<i>3D-FGAT</i>	<i>3D-VAR</i>	<i>3D-FGAT</i>
SYNOP	Z	87432	1412	+0.5%	5.5	1.49	75.88	74.04
AIREP	T	647906	192578	-5.1%	0.08	0.1	1.13	1.02
	U	641724	188572	-5.3%	0.16	0.16	3.05	2.76
	V	641724	188572	-5.3%	0.09	0.06	3.05	2.75
SATOB	U	163692	147380	-0.02%	-0.44	-0.46	2.78	2.79
	V	163692	147380	-0.02%	0.32	0.78	2.67	2.74
TEMP	Z	51028	4020	+0.1%	-1.5	-1.6	14.4	14.4
	T	131094	3974	+0.2%	0.01	0.02	1.26	1.25
	U	116986	2282	+1.1%	0.2	0.2	3.05	3.05
	V	116986	2282	+1.1%	-0.04	-0.05	3.04	3.04
	Q	119632	37886	+0.4%	-0.03	-0.03	0.82	0.82
Windprofiler	U	69644	66250	0%	0.08	0.1	3.01	2.84
	V	62838	59678	+0.2%	-0.11	-0.11	2.42	2.56
NOAA15 AMSU-A	T <sub>b</sub>	918174	712434	-1.3%	-0.05	-0.12	0.37	0.34
NOAA16 AMSU-A	T <sub>b</sub>	2461824	2102952	-0.3%	-0.13	0.22	0.35	0.36
NOAA16 AMSU-B	T <sub>b</sub>	10365349	10192964	-0.9%	0.04	0.01	2.95	2.89
NOAA17 AMSU-B	T <sub>b</sub>	5565294	5509780	+0.02%	-0.49	-0.7	2.96	2.81

\* :relative difference with respect to 3D-VAR

Table 2: Number of the rejected observations and background departure statistics in the screening of the default 3D-VAR and 3D-FGAT experiments for the whole 18-day period

It can be seen in Table 2 that the figures for 3D-VAR and 3D-FGAT are quite similar for most of the observations. As it was expected, the largest difference was found in AIREP and satellite

radiances. Apart from these observations, the differences can be attributed to the different backgrounds (at the analysis time) produced by the two analysis cycles. The quality of these backgrounds can be easily estimated with the background departures from TEMP observations (indeed it is a verification against TEMP). These values indicate that the two backgrounds at the analysis time have nearly the same quality in both systems.

It is obvious from Table 2 that AIREP reports are handled much better in 3D-FGAT than in 3D-VAR. The investigation of the vertical profiles for AIREP departures also verifies it. In Figure 4 it can be clearly seen that for temperature the 3D-FGAT background is much closer to the observations in the lower part of the troposphere. This feature corresponds to the fact that temperature near the surface can change rapidly throughout the 6 hour observation window and it can result in large errors in the computation of innovation vectors in 3D-VAR (large differences can occur between the edges and the centre of the observation window where the background state is specified). On the other hand 3D-FGAT can improve this feature a lot by computing the departures accurately. The improvement is most significant at 12 UTC (not shown) but it emerges even in the average analysis statistics (taking 00, 06, 12 and 18 UTC all together). The two wind components show similar features but the main difference can be found around the flight level (near 250 hPa). The advanced computation of innovation vector is also reflected in the screening rejection statistics because 3D-FGAT rejects a slightly less (6%) number of AIREP observations than 3D-VAR.

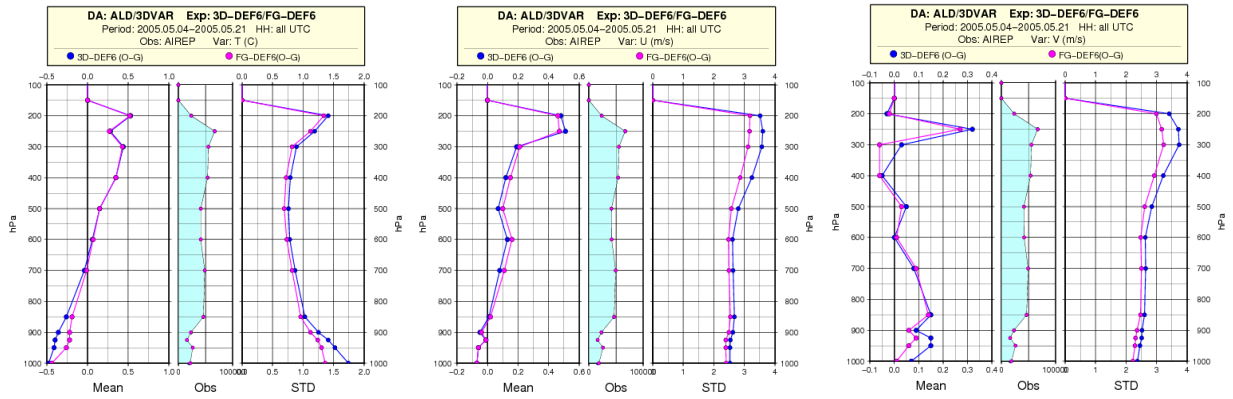


Figure 4: Background departure statistics for AIREP temperature in the 3D-VAR (blue) and 3D-FGAT (magenta) analyses (from left to right: T, U and V)

Unlike the AIREP observations, the background departure statistics for satellite radiances are not clearly better in 3D-FGAT. Regarding the mean values the background in 3D-VAR is closer to the observations than in 3D-FGAT while for the RMSE values the situation is just the opposite. Besides, the number of the rejected observations in screening shows a rather small difference.

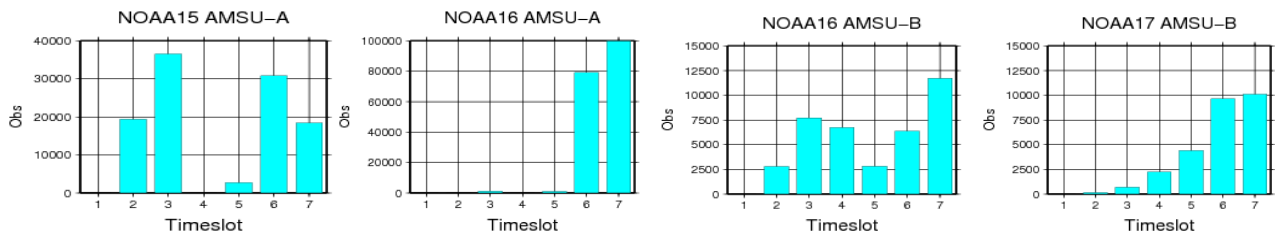


Figure 5: Temporal distribution of the active satellite radiance data for the different satellite sensors

In order to see how much the background departures in 3D-VAR and 3D-FGAT could differ at all, the temporal distribution of the satellite radiance data was investigated. It can be seen on Figure 5 that for all the sensors there are quite a large number of observations far from the analysis time



(time-slot 4), so 3D-FGAT departures are expected to be smaller than the 3D-VAR ones (both in terms of mean and standard deviation). It is interesting that in the case of NOAA16 AMSU-A albeit almost all the data are available by 2 or 3 hours later than the analysis time and yet the difference can be only seen in the mean departures.

The reason for the larger mean background departures in 3D-FGAT might be the fact that the bias correction coefficients were computed by 3D-VAR for both systems (*Randrimampianina, 2005 and 2006*). Thus, bias correction coefficients were determined from an inaccurate background departure computation and then they were applied in 3D-FGAT. However, if it is the case it is still unclear why 3D-FGAT is better in terms of standard deviation.

### 7.1.2 Comparison of forecast results

The verification for the surface parameters against SYNOP observations indicates a very small difference between 3D-VAR and 3D-FGAT (not shown). This feature is also reflected in the subjective forecast evaluation: the evolution of weather systems with regards to precipitation and cloud patterns are rather similar and the small scale differences are not systematically better or worse in either case.

The situation is different for the upper air parameters where the verification was performed against ARPEGE analyses (Figure 6). The RMSE scores of the 00 UTC 3D-FGAT forecasts are slightly better for the first 12 hours for geopotential in the upper troposphere and for U and V wind components near the 250 hPa level. This difference proved to be significant on a 90% confidence level. However, the geopotential in the lower troposphere in the 6-24 h forecast range is significantly worse in 3D-FGAT. For the relative humidity there is little difference between the two systems and the temperature forecasts are almost identical (not shown). For the 12 UTC runs the RMSE scores indicate smaller differences of the same sign as for 00 UTC except the geopotential. This parameter is worse (but not significantly) in 3D-FGAT for the first 12 hours around 250 hPa than in 3D-VAR but slightly better after 24 hours.

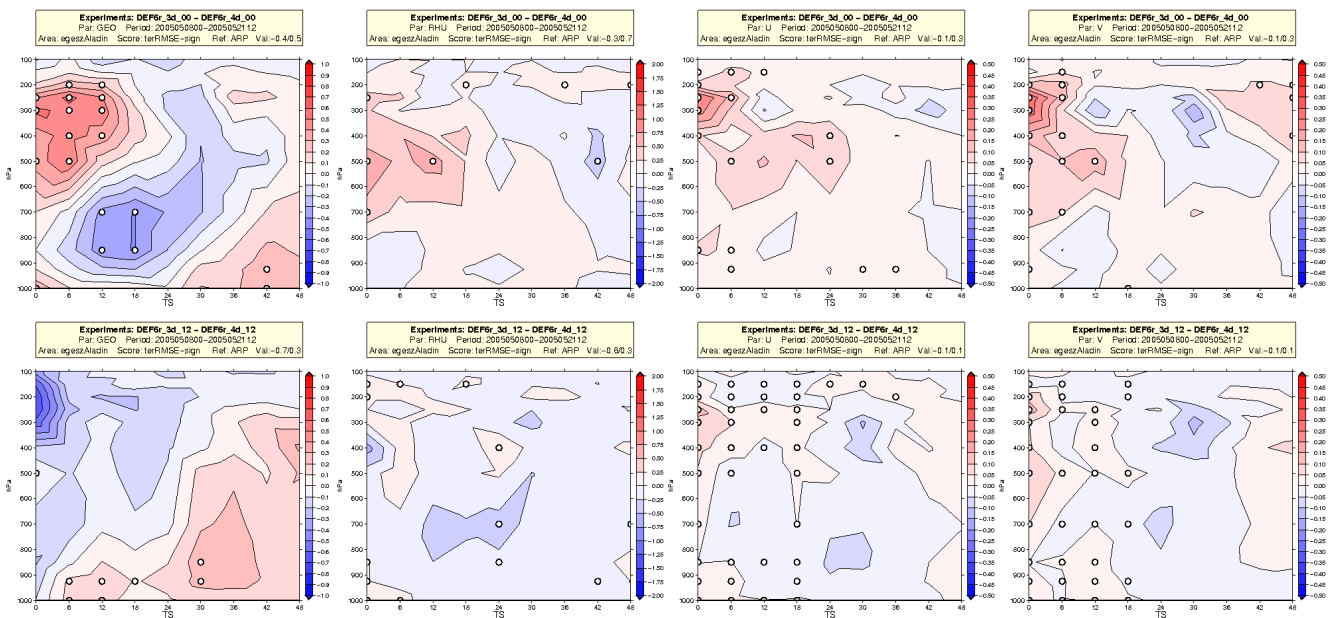


Figure 6: Difference of RMSE scores of the 00 (upper row) and 12 (lower row) UTC forecasts based on 3D-VAR and 3D-FGAT. Red shades indicate that 3D-FGAT is better, while blue shades indicate the opposite. White circles show that the difference is significant on a 90% confidence level. The verification was based on ARPEGE analyses. The figure order is the following (from left to right): Z, RHU, U and V.

The bias scores of the upper air parameters show only small differences in temperature, U and V, but a larger difference can be seen for geopotential and relative humidity (Figure 7). An interesting feature is that for both these latter parameters the bias scores indicate just the opposite as the RMSE scores: where 3D-FGAT is better in terms of RMSE there 3D-VAR is better in terms of bias and vice versa. It has to be mentioned that there is a noisy pattern for geopotential in Figure 7 around 200 hPa. It was verified that this is the consequence of visualizing the difference of the absolute values of the bias scores (the bias difference itself resulted in rather smooth fields - not shown).

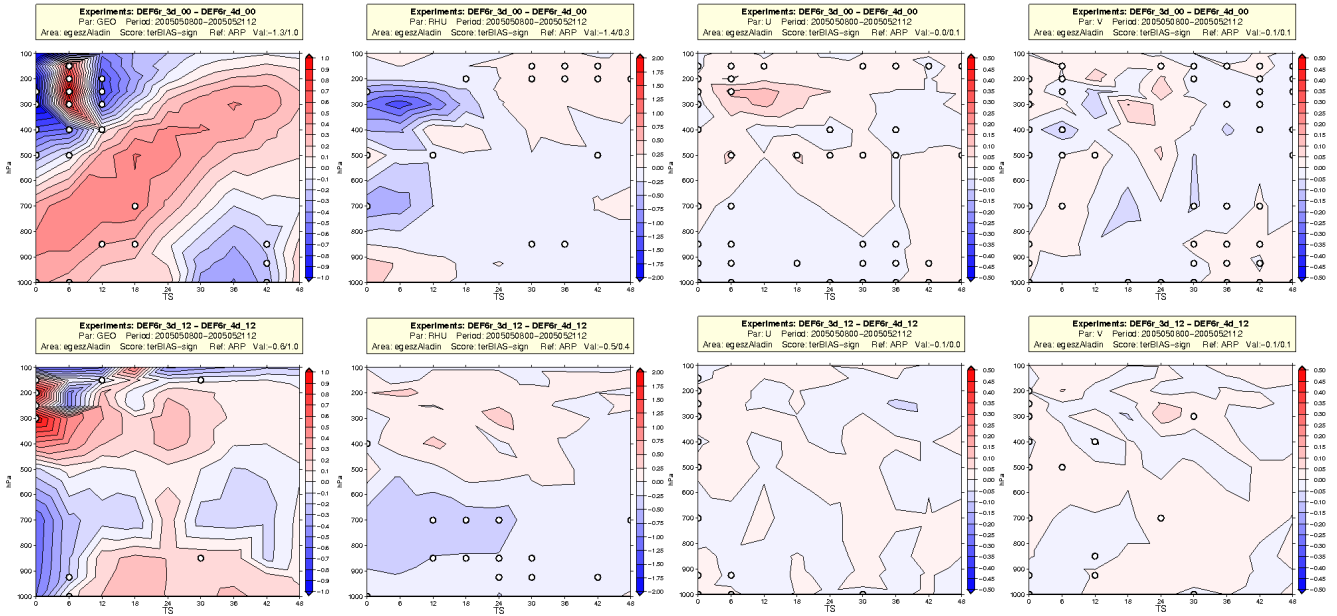


Figure 7: Difference of absolute value of bias scores of the 00 (upper row) and 12 (lower row) UTC forecasts based on 3D-VAR and 3D-FGAT. Red shades indicate that 3D-FGAT is better, while blue shades indicate the opposite. White circles show that the difference is significant on a 90% confidence level. The verification was based on ARPEGE analyses. The figure order is the following (from left to right): Z, RHU, U and V.

The results for U and V can for the 00 UTC runs be directly attributed to the effect of AIREP data but the case of geopotential is not straightforward. Although it can be explained as a consequence of the improved temperature usage for AIREP in 3D-FGAT (since geopotential is strongly linked to temperature), but then the small differences in the temperature forecasts still remain unclear. The other problem with this assumption is related to the wrong geopotential RMSE scores in 3D-FGAT near the flight level at 12 UTC. This is inconsistent with the fact that 3D-FGAT turned to be the most advanced in AIREP temperature handling at the 12 UTC analyses.

Another interesting feature is that although significantly more AIREP reports are used at 12 UTC than at 00 UTC but the difference between 3D-FGAT and 3D-VAR is smaller for the 12 UTC runs (at least for U and V). It may indicate that the usage of more wind AIREP measurements lessens the difference between 3D-FGAT and 3D-VAR in terms of forecast scores.

## 7.2 Using a shorter AIREP window

The evaluation of the reference experiments exhibited that the usage of AIREP reports in 3D-FGAT is more advanced than in 3D-VAR. However, the usage of all the AIREP reports in the 6 hour observation window is not the optimal configuration for 3D-VAR since it is optimal if only observations near the analysis time are used. Thus, another set of experiments was run with the same settings as in the reference experiments but in this case the observation window for AIREP

was shrunk to  $\pm 1$  h in both 3D-FGAT and 3D-VAR. Please note that the results presented below are only preliminary ones and the detailed evaluation of these experiments has not been finished yet.

The comparison of the 3D-FGAT and 3D-VAR forecast experiments using a  $\pm 1$  h AIREP window is shown in Figure 8. It can be clearly seen that 3D-FGAT still performs better than 3D-VAR for the 00 UTC forecasts while 3D-VAR is slightly better at the 12 UTC runs in geopotential scores. If we compare the RMSE difference patterns in Figure 8 with the reference ( $\pm 3$ h AIREP window) case (see Figure 6) we can conclude that the shortening of the AIREP window lessens the difference between 3D-FGAT and 3D-VAR. It can be also concluded that the better performance of 3D-FGAT over 3D-VAR in the reference case around 250 hPa in the first 6h is the clear consequence of the larger AIREP window.

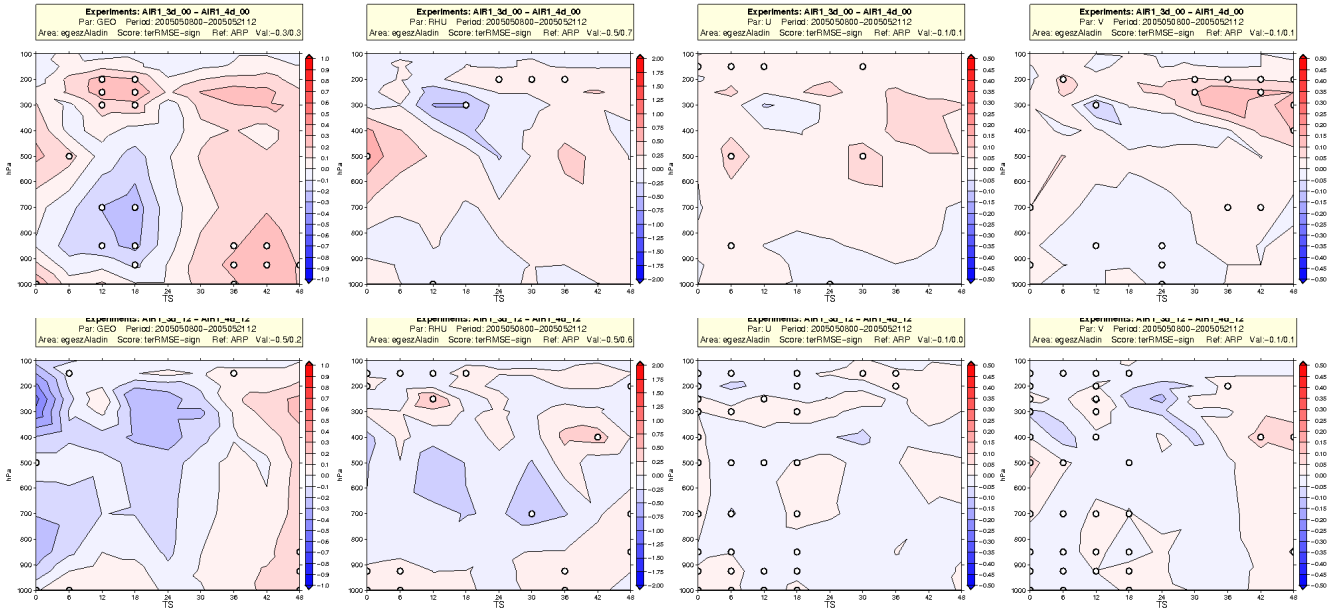


Figure 8: Difference of RMSE scores of the 00 (upper row) and 12 (lower row) UTC forecasts based on 3D-VAR and 3D-FGAT experiments with  $\pm 1$ h of AIREP window. Red shades indicate that 3D-FGAT is better, while blue shades indicate the opposite. White circles show that the difference is significant on a 90% confidence level. The verification was performed against ARPEGE analyses. The figure order is as follows (from left to right): Z, RHU, U and V.

The differences observed in Figure 8 may indicate that the AIREP window is still large enough to result in some differences between the two systems (AIREP is still distributed over 3 time-slots for 3D-FGAT in this case). Another explanation could be that this difference is caused directly by the more precise departure computation for the satellite radiance data (coming from polar orbit satellites) in 3D-FGAT. This idea could be easily verified by using no AIREP data in the experiments.

It was also investigated that how much the shortening of the AIREP window affects the performance of 3D-FGAT itself. In order to test it the 3D-FGAT experiment with the  $\pm 1$  h AIREP window was compared with the reference one. It can be seen in Figure 9 that the shortening of the AIREP window degraded the forecast results both for the 00 and 12 UTC runs. The only case where an improvement can be seen is the first 6 h of 12 UTC forecasts in around 200 hPa. An implicit consequence of these results (and it was also exhibited by upper air verification - not shown) that the reference 3D-FGAT configuration (with  $\pm 3$ h AIREP window) is even better in terms of RMSE scores than 3D-VAR with the shorter AIREP window. The only exception is the geopotential around 250 hPa in the first 6h of the 12 UTC runs.

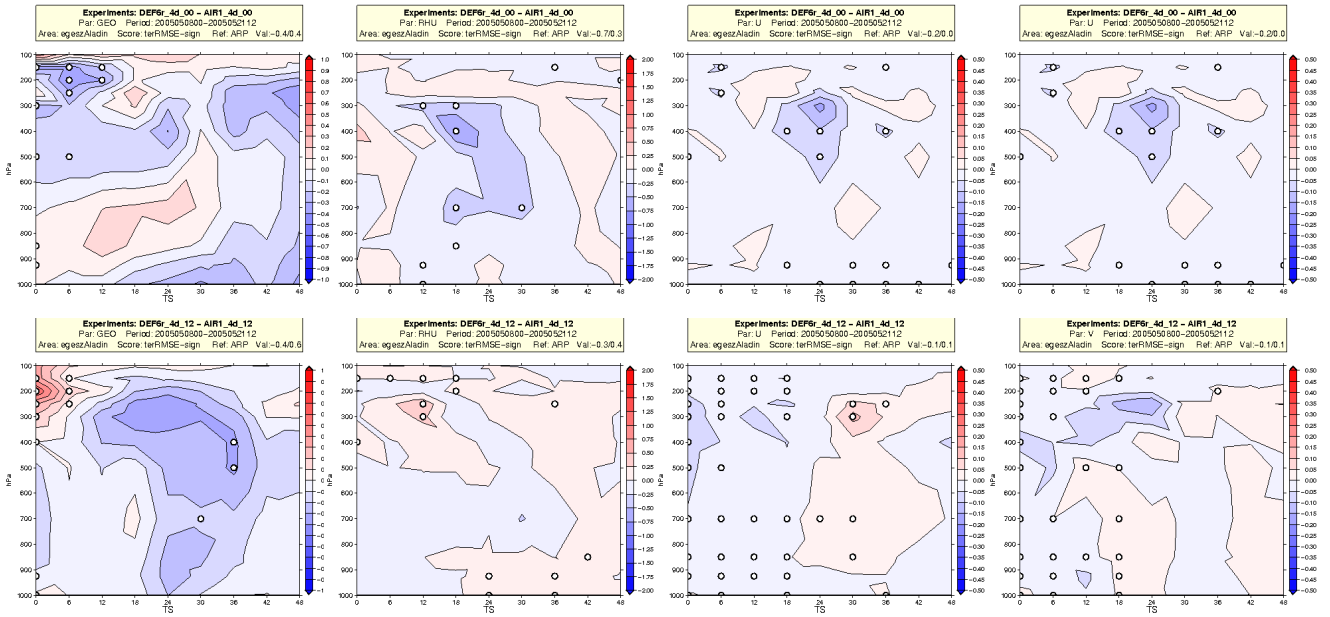


Figure 9: Difference of RMSE scores of the 00 (upper row) and 12 (lower row) UTC forecasts based on 3D-FGAT with  $\pm 1h$  and  $\pm 3h$  of AIREP window. Red shades indicate that the  $\pm 1h$  AIREP window size is better, while blue shades indicate the opposite. White circles show that the difference is significant on a 90% confidence level. The verification was performed against ARPEGE analyses. The figure order is as follows (from left to right): Z, RHU, U and V.

### 8. Using all the SYNOP reports in 3D-FGAT

In the reference experiments only one SYNOP report (the closest one to the analysis time) for a given station was used. However, the ALADIN 3D-FGAT system makes possible the usage of all the (even hourly) SYNOP reports within the observation window and in each time-slot there can be one report from a given station. As it was described in Chapter 3 it is a different case than for the fast moving platforms such as AIREP because the location of the observations is fixed now.

In the first experiment the reference set of observations was complemented by all the available SYNOP reports. It means that only geopotential was taken from SYNOP but it was used in all the possible time-slots. Thus, for a given station even 7 observed geopotential values could be used by 3D-FGAT (one per each time-slot). The forecast results based on these 3D-FGAT analyses were compared with the reference 3D-FGAT experiment (see Chapter 6.1). Both the surface (not shown) and the upper air verification scores (Figure 10) indicate that there is an extremely small difference between the two experiments with the exception of the geopotential for which the reference configuration performs significantly better for the 00 UTC runs in the 24-48 h forecast period.

In the next step the observations used in the previous experiment were complemented with all the possible 2m temperature and relative humidity observations from SYNOP reports. The forecast results now were compared with the modified reference 3D-FGAT experiment using also 2m temperature and relative humidity. The comparison of the upper air scores exhibited only a small difference between the experiments again (Figure 11). However, this time at least the scores for geopotential are more similar and there is some improvement in wind in the upper troposphere.

All things considered we can conclude that regardless of the assimilated SYNOP parameters the usage of SYNOP reports with all the possible times cannot improve the reference ALADIN 3D-FGAT configuration. According to Chapter 3 the possible reason can be that the average of the innovations for a given station does not differ too much from the innovation at the analysis time. However, this hypothesis was not checked.

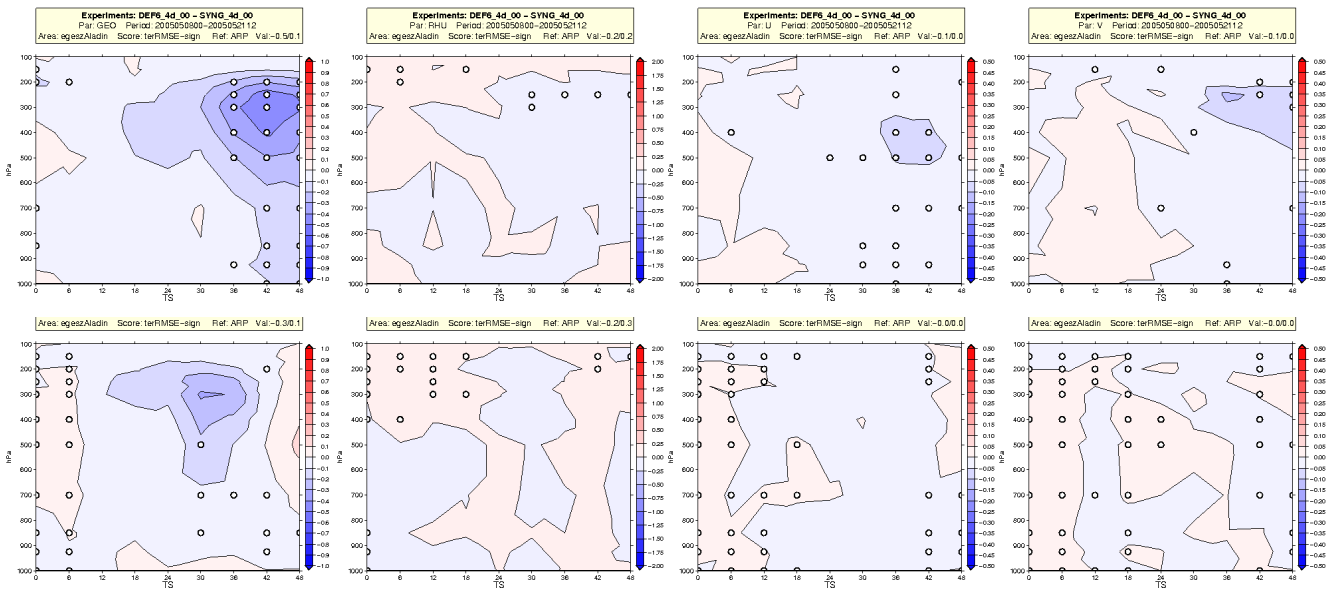


Figure 10: Difference of RMSE scores of the 00 (upper row) and 12 (lower row) UTC forecasts based on the reference system and the system using all the available SYNOP geopotential observations. Blue shades indicate that the reference system is better, while red shades indicate the opposite. White circles show that the difference is significant on a 90% confidence level. The verification was performed against ARPEGE analyses. The figure order is the following (from left to right): Z, RHU, U and V.

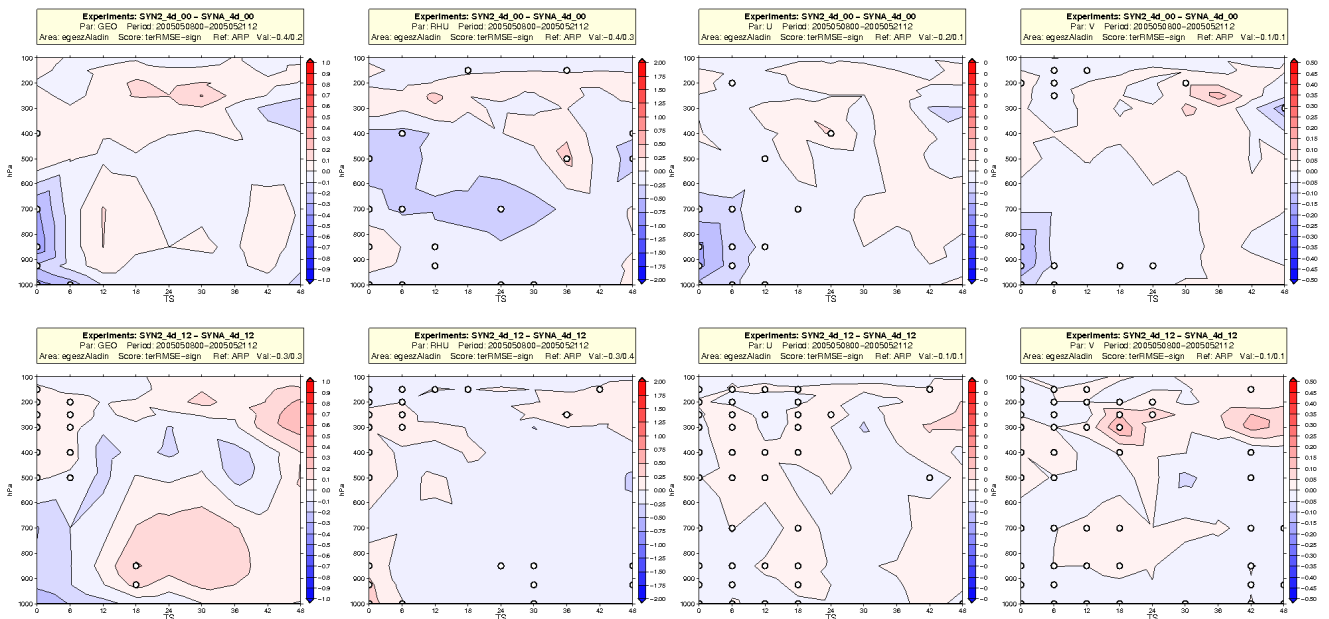


Figure 11: Difference of RMSE scores of the 00 (upper row) and 12 (lower row) UTC forecasts based on the reference system complemented with T2 and RHU2 and the system using all the available SYNOP observations. Blue shades indicate that the reference system is better, while red shades indicate the opposite. White circles show that the difference is significant on a 90% confidence level. The verification was performed against ARPEGE analyses. The figure order is the following (from left to right): Z, RHU, U and V.

## 9. Concluding remarks

In this paper the ALADIN 3D-FGAT system was tested using all the observation types available at HMS. As a first result it was verified that according to the expectations the 3D-FGAT analysis increment should be added to the trajectory at the middle of the observation window.

In the second step 3D-FGAT and 3D-VAR were compared using the same set of observations

in both systems with a  $\pm 3$ h observation window. Concerning the temporal distribution of the observations the two systems could differ only in the different usage of AIREP and satellite radiance data. The experiments revealed that the 3D-FGAT analysis is more advanced in AIREP report handling and to a less extent for satellite radiances, too. None the less the forecast results are rather similar though 3D-FGAT is a slightly better for the 00 UTC runs for some upper air parameters. A shorter ( $\pm 1$ h) AIREP observation windows was also tested and it turned out that in this case 3D-FGAT is still better than 3D-VAR at 00 UTC. It was also verified that the usage of a shorter AIREP window deteriorate the performance of 3D-FGAT in terms of forecast scores.

Finally the possible usage of all the land SYNOP reports (one in each time-slot for a station) in 3D-FGAT was also investigated. These experiments revealed that this approach cannot improve the forecast quality.

The recent research work is related to the determination of the optimal size of the observation window for SYNOP, AIREP and AMV reports in 3D-FGAT. Further tests with the use of satellite radiance bias correction coefficients computed with 3D-FGAT are also planned. The possible usage of a 3h assimilation cycle and new observation types such as SEVIRI radiances will be also considered.

**Acknowledgements** – The fruitful discussions and the strong support I received from my colleagues at the Numerical Weather Prediction Division of HMS is highly acknowledged.

## 10. References

- Dziedzic, A., 2005: Test de l'assimilation 3D-VAR FGAT sous OLIVE dans le modele ALADIN. *Internal MF report*.  
(available at: <http://www.cnrm.meteo.fr/aladin/publications/Report2005/DZIEDZIC.pdf>)
- ECMWF, 1992: ECMWF Data Assimilation – Scientific Documentation. *ECMWF Research Manual 1*, 3<sup>rd</sup> Edition
- Huang, X-Y., K. S. Morgensen and X. Yang, 2002: First-guess at the appropriate time: the HIRLAM implementation and experiments, *Proceedings for HIRLAM workshop on variational data assimilation and remote sensing*, Helsinki 22-23 January, 2002, pp 28-43.
- Randriamampianina, R., 2005: Radiance-bias correction for a limited area model, *Időjárás*, Vol. 109/3, pp. 143-155.
- Randriamampianina, R., 2006: Use and impact of the full grid AMSU-B data in the ALADIN/HU model model. *ALADIN Newsletter no. 29*.
- Soci C., 2004: 3D-FGAT in ALADIN analysis. *Internal MF report*.  
(available at: <http://www.cnrm.meteo.fr/aladin/publications/Report/Cornel2004.ps>)
- Soci C., 2004: Further tests with 3D-FGAT in ALADIN analysis. *Internal MF report*. (available at: <http://www.cnrm.meteo.fr/aladin/publications/Report/Cornel2004nov.ps>)
- Vasiliu S., 2006: An evaluation of the 3D-FGAT scheme for the ALADIN/Hungary model. *ALADIN Newsletter no. 29*.

## CONTENTS

1.	<a href="#">Introduction</a>	2
2.	<a href="#">Theoretical background</a>	2
3.	<a href="#">Theoretical aspects of observation handling in 3D-FGAT</a>	3
4.	<a href="#">Implementation of 3D-FGAT in ALADIN</a>	4
5.	<a href="#">Description of the experiments</a>	4
6.	<a href="#">The timing of the analysis increment in 3D-FGAT</a>	5
7.	<a href="#">Comparing 3D-FGAT with 3D-VAR</a>	7
7.1	<a href="#">Reference experiments</a>	7
7.1.1	<a href="#">Comparison of observation handling</a>	7
7.1.2	<a href="#">Comparison of forecast results</a>	9
7.2	<a href="#">Using a shorter AIREP window</a>	10
8.	<a href="#">Using all the SYNOP reports in 3D-FGAT</a>	12
9.	<a href="#">Concluding remarks</a>	13
10.	<a href="#">References</a>	14